Article

Performance Improvement of an Electric Vehicle Charging Station Using Brain Emotional Learning-Based Intelligent Control

Sherif A. Zaid [1,*], Hani Albalawi [1,2], Aadel M. Alatwi [1,3] and Atef Elemary [4]

[1] Electrical Engineering Department, Faculty of Engineering, University of Tabuk, Tabuk 47913, Saudi Arabia; halbala@ut.edu.sa (H.A.); adalatawi@ut.edu.sa (A.M.A.)
[2] Renewable Energy and Environmental Technology Centre, University of Tabuk, Tabuk 47913, Saudi Arabia
[3] Industrial Innovation and Robotic Center (IIRC), University of Tabuk, Tabuk 47731, Saudi Arabia
[4] Electrical Engineering Department, Faculty of Engineering, Jizan University, Jizan 45124, Saudi Arabia; aelemary@jazanu.edu.sa
[*] Correspondence: shfaraj@ut.edu.sa

Abstract: Electric vehicle (EV) charging facilities are essential to their development and deployment. These days, autonomous microgrids that use renewable energy resources to energize charging stations for electric vehicles alleviate pressure on the public electricity grid. Nevertheless, controlling and managing such charging stations' energy is difficult due to the nonlinearity and irregular character of renewable energy sources. The current research recommends using a Brain Emotional Learning Intelligent Control (BELBIC) controller to enhance an autonomous EV charging station's performance and power management. The charging station uses a battery to store energy and is primarily powered by photovoltaic (PV) solar energy. The principles of BELBIC are dependent on emotional cues and sensory inputs, and they are based on an emotion processing system in the brain. Noise and parameter variations do not affect this kind of controller. In this study, the performance of a conventional proportional–integral (PI) controller and the suggested BELBIC controller is evaluated for variations in solar insolation. The various parts of an EV charging station are simulated and modelled by the MATLAB/Simulink framework. The findings show that, in comparison to the conventional PI controller, the suggested BELBIC controller greatly enhances the transient responsiveness of the EV charging station's performance. The EV keeps charging while the storage battery perfectly saves and keeps steady variations in PV power, even in the face of any PV insolation disturbances. The suggested system's simulation results are provided and scrutinized to confirm the concept's suitability. The findings validate the robustness of the suggested BELBIC control versus parameter variations.

Keywords: brain emotional learning intelligent control; electric vehicle; charging station; PV

1. Introduction

In the pursuit of environmental sustainability, one of the main issues of this period that is becoming more and more concerning is global warming [1,2]. The progressive increase in the planet's average surface temperature is referred to as "global warming", which is mostly caused by an intensified greenhouse effect. The Earth's surface heats naturally due to the greenhouse effect. However, as a result of modern industrial developments that include the burning of fossil fuels (such as natural gas, oil, and coal), industrial processes, and deforestation, the amount of greenhouse gases in the environment has significantly increased. Twenty-five per cent of the world's greenhouse gas emissions come from transportation [3,4]. Conventional vehicles are often powered by fossil fuels, which emit copious volumes of gas. EVs have recently been launched to replace conventional

automobiles [5]. Compared to traditional vehicles, EVs are more efficient, require less maintenance, produce less pollution, and produce less noise.

An essential facility for the development of EVs is their charging stations. A few of the issues that still need to be resolved are related to the charging stations' architecture, how long it takes to charge an EV, and how these stations affect the existing power supply. The charging period of a certain EV can be significantly lowered to a few minutes with rapid charging approaches [6]. These techniques, however, put a strain on the electricity supply and increase demand for power. Several problems arise as a result, including excess loading, jerking of the voltage, and instability, especially if multiple EV stations are linked to the grid at the same time [7]. One solution to these problems is to upgrade the electrical system, although this would be costly. Employing an energy storage device to work as a shield between the EV charging station and the electricity grid is an even better tactic [8]. With the installation of energy storage devices, the utility grid will become less stressed, but challenges will still arise from the projected increase in EV charging stations in the coming years. Typically, traditional sources like coal and fossil fuels provide the electrical energy needed for the charging stations of EVs [9]. Therefore, the argument that EVs are environmentally friendly may not be credible. Thus, to highlight the benefits of EVs for the environment, renewable sources should be employed for EV stations.

The most typically used renewable sources for charging stations are solar, wind, and biogas energy systems [10]. PV solar systems are more user-friendly and efficient than wind energy systems. For EV charging stations, PV power is consequently more appealing. Numerous research studies have addressed PV-based charging stations [11]. One study proposed an idea for a PV-supplied EV charging station [12]. Additionally, the study offered a mathematical model of the EV charging station and evaluated the system's response to various disturbances using simulation methods. Finally, the findings of the simulation showed that the recommended charging station was able to function without relying on the electricity network, and meet an EV's station requirements. An EV charging station supplied with a PV panel was suggested by the authors of [13]. The study addressed the construction of a PV panel, a DC-DC converter, and the application of the perturb and observe approach in order to upgrade the efficiency of the charging process. The findings of the simulation suggested that charging an electric automobile at the proposed station might be a reliable and efficient process. A crossbreed microgrid that used wind and solar electricity to power an EV charging station linked to the utility grid was the subject of research detailed in [14]. The system was simulated by research using the HOMER platform. It determined the optimum proportion of wind and solar supplies, storage capacity, and demand for EV stations to optimize their construction. The findings showed that the crossbreed microgrid had a reasonable payback period and was technically feasible. Also, the research examined the possible advantages of the crossbreed microgrid, which included enhancing energy security, reducing emissions of CO_2, and fostering local economic growth through the induction of green jobs. Ref. [15] proposed the use of electric railway power to charge EVs with an autonomously sourced microgrid that employs the public utility as an alternate. Ref. [16] employed a multi-level DC/DC converter to combine PV arrays and a battery bank to incorporate PV power into an EV fast charging station. This system aimed to ease some of the stress on switching devices. However, output capacitor voltage balance still needs to be taken into consideration.

Recently, the BELBIC, a novel controller, has been proposed [17]. It has excellent resilience, ease of use, efficacy, and adaptability in terms of choosing the right emotional cues and sensory inputs for the right application. The limbic system computational model in the human brain served as the inspiration for this controller [18]. It has several uses in electric power systems, automobile systems, and spacecraft [19,20]. A few recently published papers in the suggested field exist. An autonomous wind/photovoltaic microgrid using an optimum maximum power point controller was presented in ref. [21]. Energy management and peak power tracking were supplied via the controller. Despite being straightforward, the system's efficiency was not guaranteed. An isolated power system

fueled by an autonomous wind-photovoltaic battery microgrid was shown in reference [22]. It made use of the SEPIC converter and the traditional PID controller. Nonetheless, there was a steady-state inaccuracy in the load voltage, and a decent time response from the system. An intelligent energy management controller was shown in ref. [23]. It made use of a mixed approach combining fractional-order PID and fuzzy logic. Both DC and AC loads were guaranteed constant output power by the suggested controller. The harmonics of the voltage and current, however, were considerable. Furthermore, ramp disturbance resistance was not verified for the suggested microgrid. Reference [24] proposed the utilization of multi-agent deep reinforcement learning for multi-mode plug-in hybrid EV energy management. Though the energy saving was about 4%, tedious computations and a complex system were involved.

The irregular behavior of EVs affects charging stations in several ways, including in terms of grid stability, long wait times, charging efficiency, and the availability of charging slots. Operators of charging stations can counteract these impacts by putting in place improved scheduling algorithms, real-time charging session monitoring, incentives for users to follow proper charging procedures, and enhanced billing systems that guarantee correctness and openness. Furthermore, improvements in vehicle-to-grid integration and smart grid technology can optimize charging habits and raise the general effectiveness and dependability of EV charging infrastructure. This issue has not been considered in our study; however, it is recommended for future work.

The basic problem that needs to be addressed is the management of the energy in the system, hence achieving the load requirements represented by the charging EVs, ultimately utilizing the generated solar PV energy, and finally storing the remaining energy in the storage batteries. The milestone for achieving perfect energy management is the control of the bidirectional converter that manages the charging processes of the storage batteries. Usually, these types of converters are considered complex systems from the control point of view. As the detailed modelling of these converters is hard, traditional controllers exhibit limited performance when applied to power electronics converters [25]. Therefore, there exists a motivation to apply one of the modern control technologies, such as BELBIC, to a PV-powered EV charging station. An implementation of the BELBIC controller for managing and controlling an autonomous EV charging station powered by solar energy is shown in this paper. A unidirectional converter is used to charge the EV, whereas a two-way converter is utilized to charge and discharge the storage system. The optimal BELBIC controllers serve as the foundation for the control and power management of the suggested charging station. The essential goals of the microgrid are to control the voltage of the DC link, manage system energy, and regulate the charging of storage batteries and electric vehicles. Additionally, analyses of the responses of the suggested BELBIC controller and the conventional PI controller were conducted. Matlab was implemented to develop and simulate the newly introduced EV charging station. The contributions of this study were:

- A BELBIC controller was implemented to enhance the functionality of the suggested EV charging station.
- The suggested system's performance using the BELBIC controller versus the traditional PI were compared.
- The performance of the controllers was evaluated under various solar insolation and load disturbances.
- The impacts of fluctuations in the solar insolation on the microgrid's response were discussed and analyzed by modelling the suggested system using MATLAB (version R2023a).
- The suggested control system's durability was explored against the parameter uncertainty of the system.

The present study is structured as follows: Section 2 discusses and models the proposed EV charging station; Section 3 provides the suggested control system for the

EV charging station; Section 4 covers the simulation findings; and Section 5 presents the conclusions.

2. Modelling and Description of the Suggested Station

The planned EV charging station is illustrated in Figure 1. The station is a self-sufficient microgrid that obtains its electricity from photovoltaic (PV) solar panels. However, the quantity of energy created fluctuates according to several climatic conditions, including rainfall, dust, humidity, and sun insolation. These elements determine the discontinuity in the PV's output energy.
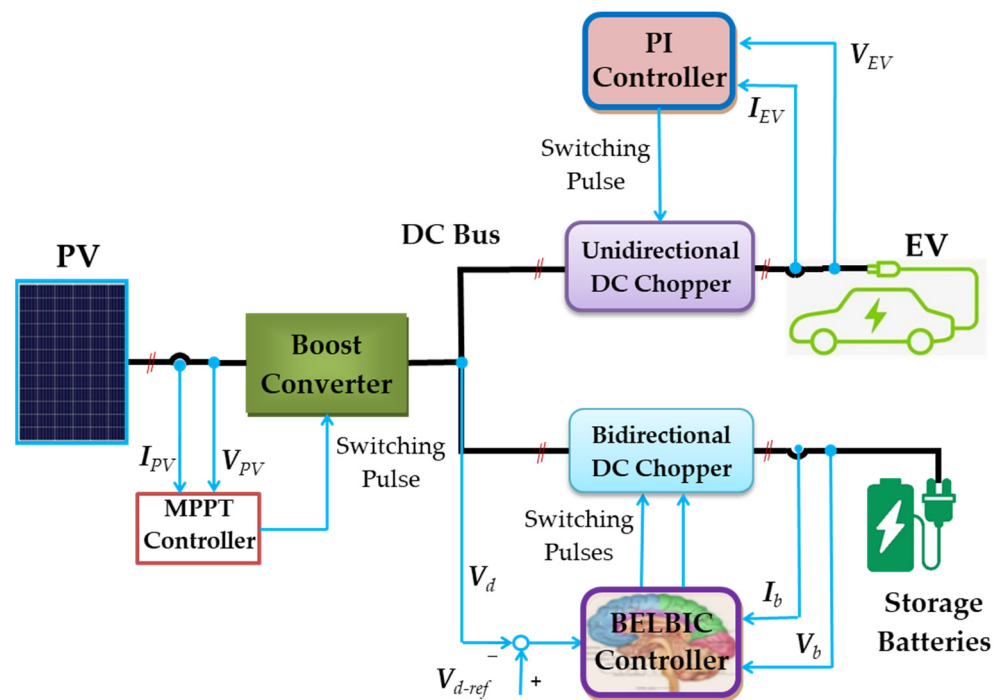

Figure 1. The investigated PV charging station.

For most customers, this energy discontinuity poses an issue, as it is unsuitable for several loads. Thus, the problem of intermittent energy supply is usually addressed by storing batteries. At the PV terminals, a step-up chopper is connected. The objective of this chopper is to use the maximum power of the PV array by fitting the PV output voltage to the bus DC voltage. The storage batteries and the EV are attached to the DC bus via two charging converters. It is usually made up of DC choppers. A single quadrant buck chopper is employed to regulate the electric vehicle battery's charging process. In contrast, the energy storage converter functions as a two-way DC chopper. Its job is to control the storage battery charging procedures. Also, the energy storage converter helps regulate the voltage of the DC bus in response to variations in the load represented by the EV and solar irradiation. A detailed design of the capacity of the renewable energy and storage devices in the proposed system was introduced by the authors in Refs. [4,12]. The modeling and fundamentals of the workings of charging converters are covered in the next sections.

2.1. PV Model

To provide the appropriate voltage for the boost converter and, ultimately, produce the necessary DC link voltage, the PV panel is composed of one series module and one parallel module. Table 1 provides the PV array's specifications when the sun's insolation level is equal to 1 kW/m^2.

Table 1. The PV panel specifications with full solar power.

Item	Value
Maximum power	120 W
Voltage and current for maximum power (V_{pmax}, I_{pmax})	17.33 V, 6.93 A
Number of series and parallel cells	360 series, and 10 parallel
Short circuit current	7.49 A
Open circuit voltage	21.6 V
Temperature	25°

The detailed PV array model is given in [26,27]. However, a typically simplified and somewhat accurate model of the PV array is shown in Figure 2a. The PV panel has the electrical characteristics presented in Figure 2b.
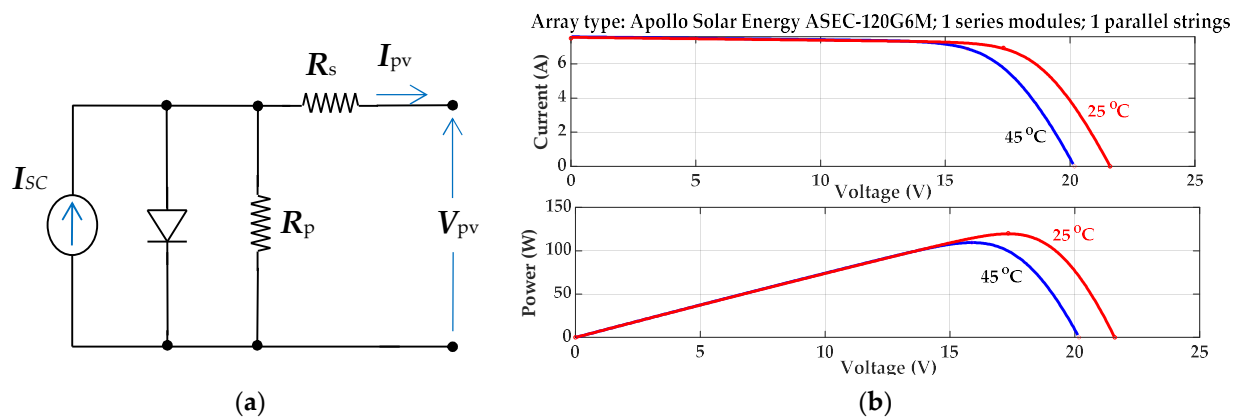
Figure 2. The model of the PV panel (**a**) equivalent circuit [28], and (**b**) PV characteristics.

(V_{pv}, I_{pv}) are the PV voltage and current; (R_s, R_p) are the panel equivalent series and parallel resistances; and (I_{SC}) is the short circuit current.

2.2. Step-Up Chopper Model

A schematic for the basic step-up chopper is shown in Figure 3a in its conventional format. The input of the chopper is the PV terminals, and its output is connected to the DC bus. Different models have been implemented for this chopper; however, the average model is the simplest and most suitable for our case. In [29], the following is the average model of a step-up chopper working in the continuous mode of operation:

$$\begin{bmatrix} V_d \\ I_d \end{bmatrix} = \begin{bmatrix} \frac{1}{1-d} & 0 \\ 0 & 1-d \end{bmatrix} \begin{bmatrix} V_{pv} \\ I_{pv} \end{bmatrix} \tag{1}$$

where (d) is the duty cycle ratio; (V_d, I_d) are the DC bus average voltage and current; and (L_b) is the step-up converter inductance.

2.3. Step-Down Chopper Model

The converter topology is shown in Figure 3b. It consists of one IGBT (Q_3) and a smoothing filter. The storage battery is modelled as an internal voltage with a series resistance. The IGBT is modulated by the controller to charge the EV battery with a certain current, achieving full charging. When switch Q_3 is activated and the antiparallel diode acts as a flywheel, it operates in the buck charging phase. The equivalent circuits during each mode are presented in Figure 4a,b. The model equations may be derived as follows:
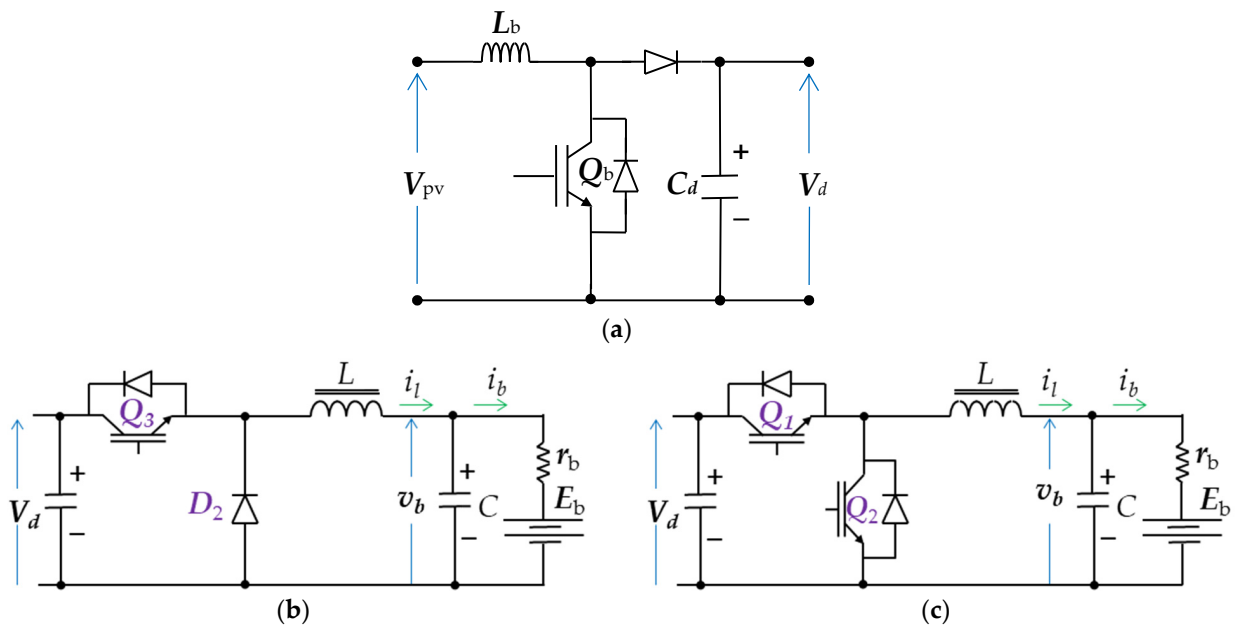
Figure 3. The basic (**a**) step-up chopper circuit, (**b**) step-down chopper circuit, and (**c**) two-way chopper circuit.
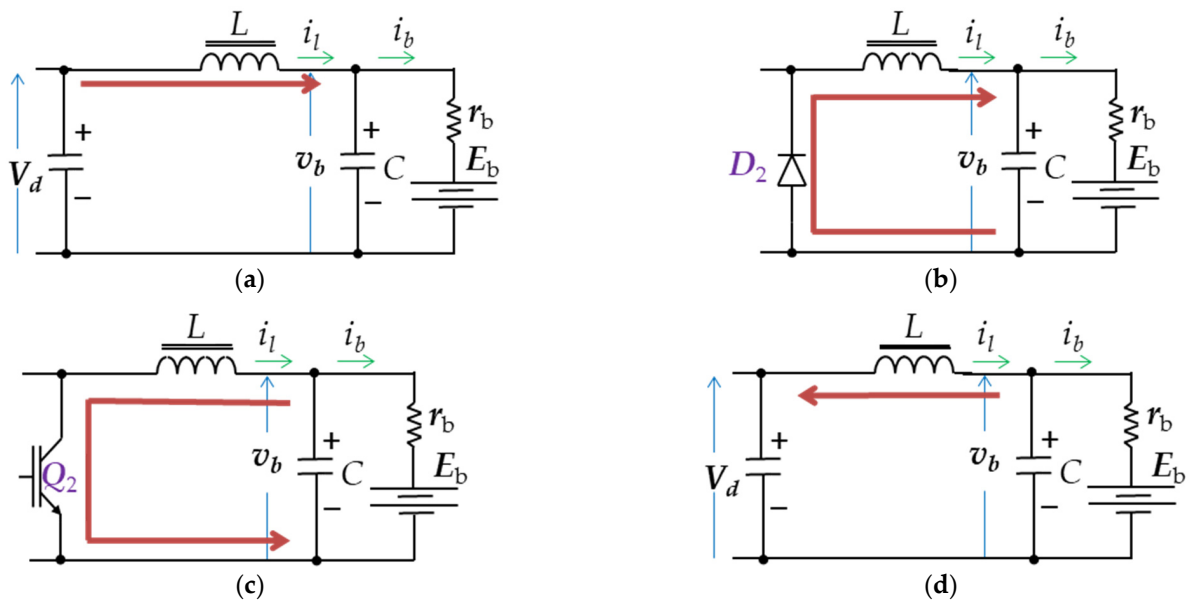

Figure 4. The equivalent circuits of the converters (**a**) mode #1, (**b**) mode #2, (**c**) mode I, and (**d**) mode II.

Mode (1): Q_3 is on.

Referring to the equivalent circuit shown in Figure 4a, the KVL equations can be written as:

$$C\frac{dv_b}{dt} = i_l - \frac{v_b - E_b}{r_b}, \quad L\frac{di_l}{dt} = -v_b + V_d \qquad (2)$$

where (L, C) are the filter inductance and capacitance; (E_b, r_b) are the battery internal voltage and resistance; and (i_l) is the inductor current.

Mode (2): Q_3 is off.

Referring to the equivalent circuit shown in Figure 4b, the KVL equations can be written as:

$$C\frac{dv_b}{dt} = i_l - \frac{v_b - E_b}{r_b}, \quad L\frac{di_l}{dt} = -v_b \qquad (3)$$

Equations (2) and (3) can be written in matrix form, as presented in Equation (4). Hence, the converter's state-space model is provided as follows:

$$X = \begin{bmatrix} i_l \\ v_b \end{bmatrix}, \quad \dot{X} = \begin{bmatrix} 0 & \frac{-1}{L} \\ \frac{1}{C} & \frac{-1}{r_b C} \end{bmatrix} X + \begin{bmatrix} \frac{V_d}{L} \\ 0 \end{bmatrix} Q_3 + \begin{bmatrix} 0 \\ \frac{E_b}{r_b C} \end{bmatrix} \tag{4}$$

where (Q_3) is the modulating function of the IGBT.

2.4. Two-Way Converter Model

The converter topology is shown in Figure 3c. It consists of two IGBTs (Q_1, Q_2) and a smoothing filter. Its input is the DC link of the station; however, its output is the storage battery. The bidirectional converter can absorb or generate electrical power [30]. It absorbs power when charging the battery. However, it generates power when the battery is discharging. It is thought that the filter inductance is sufficiently large to hold on to adequate energy to manipulate the charging process of the storage battery. As a result, continuous conduction operation is guaranteed. The converter operates in two phases: the discharging phase and the charging phase. When switch Q_1 is on and Q_2 is modulated in the discharging phase, the battery is discharged via the bidirectional converter. On the other hand, when switch Q_1 is modulated and switch Q_2 is on, it operates in the charging phase, in which the battery is charging. The converter's state-space model in the charging phase is typical, as in Equation (4). The equivalent circuits, during each mode of the discharging phase, are presented in Figure 4c,d. The model equations may be derived as follows:

Mode (I): Q_2 is on.

Referring to the equivalent circuit is shown in Figure 4c, the KVL equations can be written as:

$$C\frac{dv_b}{dt} = i_l - \frac{v_b - E_b}{r_b}, \quad L\frac{di_l}{dt} = -v_b \tag{5}$$

Mode (II): Q_2 is off.

Referring to the equivalent circuit shown in Figure 4d, the KVL equations can be written as:

$$C\frac{dv_b}{dt} = i_l - \frac{v_b - E_b}{r_b}, \quad L\frac{di_l}{dt} = -v_b + V_d \tag{6}$$

Equations (5) and (6) can be written in the matrix form, as presented in Equation (7). Therefore, the model in the discharging phase is as follows:

$$\dot{X} = \begin{bmatrix} 0 & \frac{-1}{L} \\ \frac{1}{C} & \frac{-1}{Cr_b} \end{bmatrix} X + \begin{bmatrix} \frac{-V_d}{L} \\ 0 \end{bmatrix} Q_2 + \begin{bmatrix} \frac{V_d}{L} \\ \frac{E_b}{Cr_b} \end{bmatrix} \tag{7}$$

where (Q_2) is the modulating function of the IGBT.

3. Control System Description

The control system of the proposed EV charging station must achieve the following objectives:

- Catch the maximum power output from the PV panel.
- Regulate the charging process for the EV.
- Regulate the DC bus voltage.
- Regulate the charging processes of the battery storage.

To obtain these objectives, the control system is formed by three controllers. The first controller, which is the main controller, is the storage battery controller. It also regulates the DC bus voltage level. Figure 5a presents the details of that controller. It has two control loops, namely the current loop and the voltage loop. Nevertheless, the outer loop is the DC bus voltage loop, which is controlled using a BELBIC controller. The controller generates the setpoint signal for the current loop. On the other hand, the innermost loop is the current loop, which must be faster than the outer loop for stable operation [31]. Hence, the current

loop controller is selected to be a bang-bang controller. The second controller is the EV charging controller. It has, as shown in Figure 5b, two nested loops like the storage battery controller. However, the controllers are simply proportional–integral controllers. The third one is the maximum power point controller of the PV panel. The control action is achieved by measuring the PV voltage and current as inputs. Then, a procedure for the maximum power point controller is implemented to generate the step-up converter duty ratio, as shown in Figure 5c. The following section discusses the algorithm of the BELBIC controller.
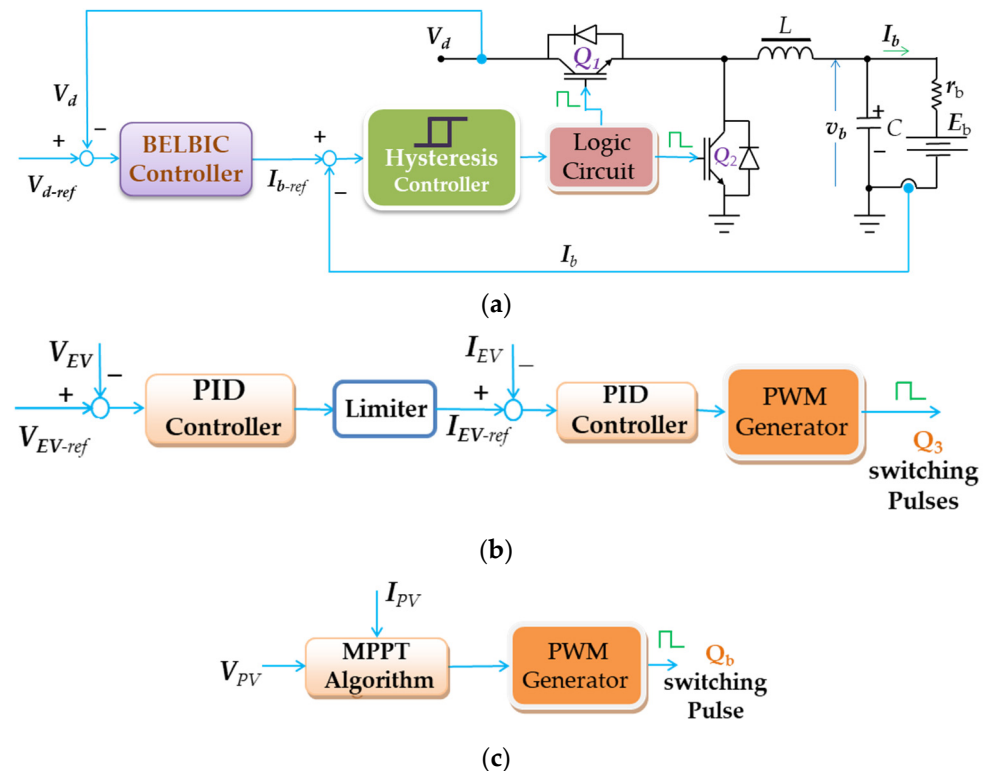

(a)

(b)

(c)

Figure 5. The EV charging station controllers: (**a**) storage battery charger controller, (**b**) EV charger controller, and (**c**) maximum power point regulator.

Proposed BELBIC Controller

A computer model of the limbic system's cognitive processes related to emotion processing was created by the BELBIC control system [32]. Figure 6a shows the model of the suggested BELBIC structure. In essence, the BELBIC approach is an action creation mechanism that takes emotional cues and sensory inputs into account. Control engineering judgment informs the selection of sensory inputs (feedback signals) in every specific application, while the performance objectives of that application influence the selection of emotional cues. These can generally be vector-valued quantities. In this study, one sensory input and one emotional signal (stress) have been taken into consideration for the purpose of illustration [33,34]. There are many nods in various model parts in Figure 6a, and the same mathematical formulas are used to simulate each one of them. An illustration of emotional learning in the brain is plotted in Figure 6b. After receiving sensory input (S), the thalamus preprocesses the incoming information. Analyzed input signals reach the sensory cortex and amygdala. The emotional signals (ES) are utilized to compute the outcomes utilizing the amygdala and orbitofrontal cortex. The final choice is obtained by deducing the orbitofrontal cortex and amygdala outputs [35]:

$$MO = \sum_{l} A_l - \sum_{l} O_l \tag{8}$$
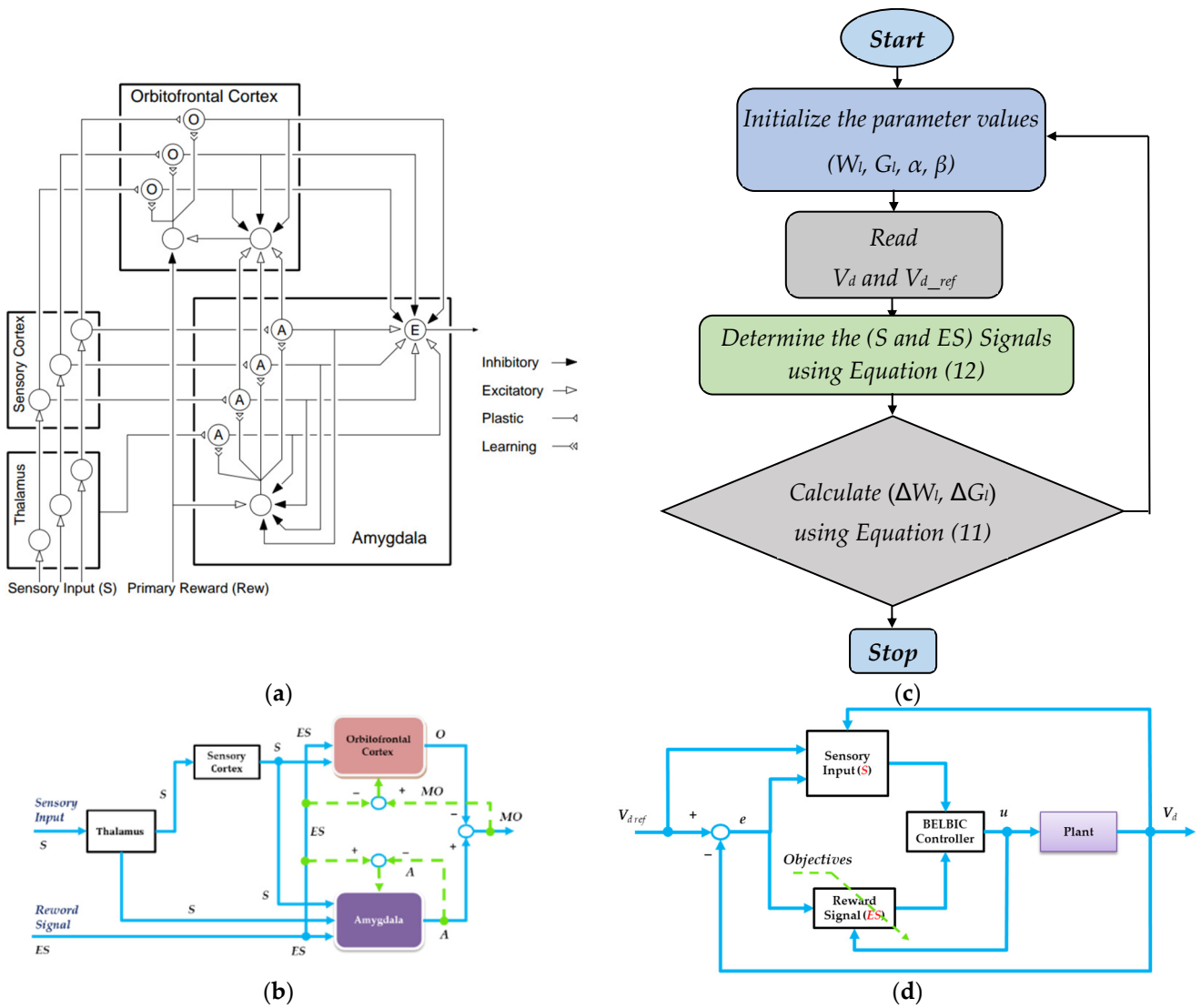
where l is the number of sensory inputs.

Figure 6. (**a**) The emotional learning model; (**b**) The BELBIC controller's architecture; (**c**) The intended plant's incorporation of the BELBIC controller; and (**d**) The BELBIC controller's flowchart.

Every input is intended for Node A. Additionally, the thalamus system sends the greatest stimulus–response signal to the A_{th} node in the amygdala system through a pathway known as the thalamic link.

$$A_{th} = MAX\{S_l\} \tag{9}$$

The amygdala and orbitofrontal cortex's outputs are calculated by summing up all of their respective nodes, with each node's outputs being derived as follows:

$$\begin{bmatrix} A_l \\ O_l \end{bmatrix} = S_l \begin{bmatrix} G_l \\ W_l \end{bmatrix} \tag{10}$$

where (G_l and W_l) are the weighting parameters of the amygdala and orbitofrontal cortex, respectively. These weighting parameters are updated regularly using:

$$\begin{bmatrix} \Delta G_l \\ \Delta W_l \end{bmatrix} = \begin{bmatrix} \alpha S_l \max(0,\ ES - \sum_l A_l) \\ \beta S_l \max(\sum_l A_l - ES) \end{bmatrix} \tag{11}$$

where (α and β) are known as the rate of learning of the two units. The complexity of the model under consideration and the required response determine which of S and ES to choose. The (S and ES) signals are implemented based on the following cost functions:

$$\begin{bmatrix} S_l \\ ES \end{bmatrix} = \begin{bmatrix} J\left(e,\ V_d,\ V_{d\_ref}\right) \\ f(e,u) \end{bmatrix} \tag{12}$$

where (e) is the DC bus voltage error, (V_d) is the plant output, (V_{d_ref}) is the reference signal, and (u) is the control effort output. The integration of the BELBIC controller with the proposed plant is illustrated in Figure 6c. A flowchart for the controller is presented in Figure 6d. The BELBIC parameters have been adjusted using a variety of techniques [36]. This work used a heuristic approach to determine the BELBIC parameters.

4. Simulation Results and Discussion

Matlab was used to simulate the suggested EV charging station displayed in Figure 1 to verify the idea stated in this research. The technical information about the EV charging station parts was as follows: the storage battery was (Lead-acid, 65 Ah, 12 V) and initially charged to 80%; the EV battery was (Nicle-cadmium, 6.5 Ah, 15 V) and initially charged to 60%; and the passive components were (L = 2000 μH, C_d = 3300 μF). Figure 7 shows the charging station response using the suggested BELBIC controller in comparison to the traditional PI controller for ramp and step variations in solar irradiation.

The solar irradiation variation is shown in Figure 7a. It has ramp changes with varying slopes, as well as large and medium stairs. The PV voltage responses for both controllers are shown in Figure 7b,c. Figure 7d,e depict the PV current responses for both controllers according to the ramp and stair changes in solar insolation level. The PV current values coincide with the conditions of the maximum power point. The level of solar radiation decreases to null during the interval ($8 \text{ s} \leq t \leq 9 \text{ s}$), which results in zero PV output voltage and current. The responses of the voltage of the DC bus for BELBIC and conventional PI controllers corresponding to the variations in insolation level are shown in Figure 7f,g. Figure 7f illustrates how closely the DC bus voltage for the BELBIC controller matches its reference value with zero steady-state error. On the other hand, the PI controller responses have zero steady-state error except at some periods, the ramp periods. This phenomenon is well known for PI controllers having a poor response with non-step inputs. Nonetheless, the reaction of the BELBIC controller has the least overshoot ($\leq 6\%$). Conversely, the response of the conventional PI controller has an overshoot of less than 12%. Thus, 50% represents the drop in the overshoot. Furthermore, utilizing the BELBIC controller, the DC bus voltage has a reduced settling time of ≤ 0.08 s. On the other hand, ≤ 0.2 s is the settling time using the PI controller. Therefore, the decrease in DC bus voltage settling time is 60%. The aforementioned improvements show that the proposed BELBIC controller considerably enhances system transient response. Additionally, it is seen that polluted ripples are absent from the DC bus voltage waveshape when using the BELBIC controller, compared to the response when utilizing the traditional PI controller.

For the PV's power, the storage battery's power, and the power of the EV's battery, Figure 8 contrasts the suggested BELBIC controller with the traditional PI controller. However, the responses from the controllers and the way they monitor the PV's maximum power point level do not change. The PV power responses for both controllers are shown in Figure 8a,b, respectively. At the first second, [1 s < t < 2 s], the insolation increases linearly, and so does the generated PV energy. The PV energy generated may therefore be used to fully charge the battery of the EV and save any leftover energy in the storage battery. Then, the solar irradiation in the next second, from [2 s to 3 s], is 100%, which is enough to charge the EV and store the rest in the storage battery. In the next three to four seconds, the insolation decreases linearly to 70% insolation. Hence, the stored energy decreases linearly while the EV charging is constant. At the interval [4 s < t < 5 s], the sun's insolation is constant at 70%. As a result, the PV power is steady and capable of charging the storage

battery in addition to the EV. During the next period, from [5 s to 6 s], the insolation drops to 25%. In this period, the generated PV energy is not enough to keep the reserve in the storage battery and charge the EV battery. In the next interval [6 s < t < 8 s], the insolation is 65%, which is insufficient to keep the reserve in the storage battery and charge the EV battery. At the interval [8 s < t < 9 s], the sun's insolation entirely disappears. Finally, the insolation steps to 100%, which is a large step. The operation returns to the previous case.
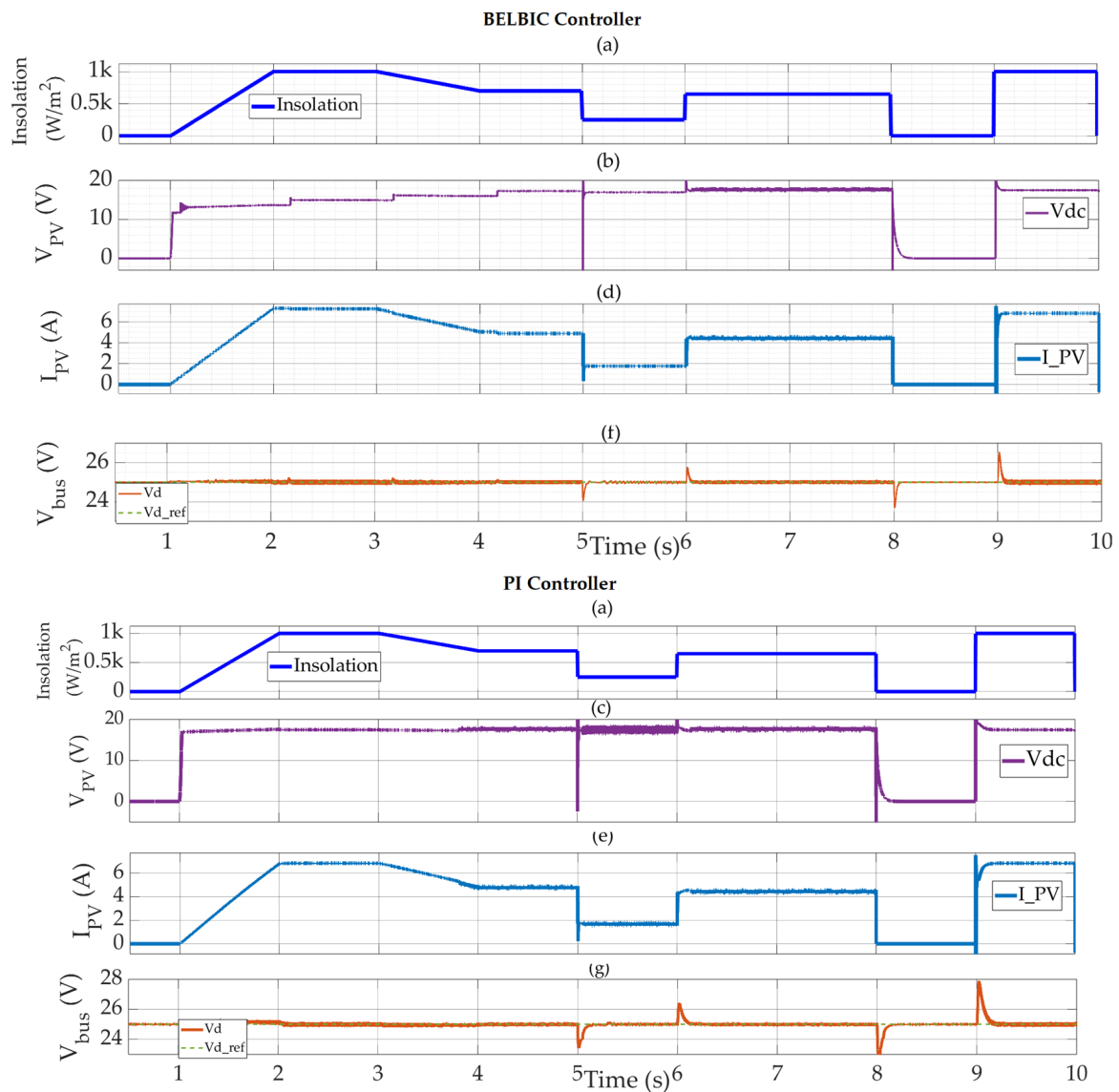

Figure 7. The performance of the EV charging station using the conventional PI controller (**a,c,e,g**) and the suggested BELBIC controller (**a,b,d,f**).

However, the transient of this large step is considerable. Consequently, no power is generated. Hence, to counteract the decrease in solar production, the storage battery empties. Also, to compensate for the drop in solar energy, the storage battery discharges, as shown in Figure 8c,d. Additionally, the radiation variations are explained by the charging and discharging processes. The two controllers are shown in Figure 8e,f, which show that the EV power remains constant in all situations. The suggested BELBIC controller, on the other hand, responds more smoothly and does not overshoot.
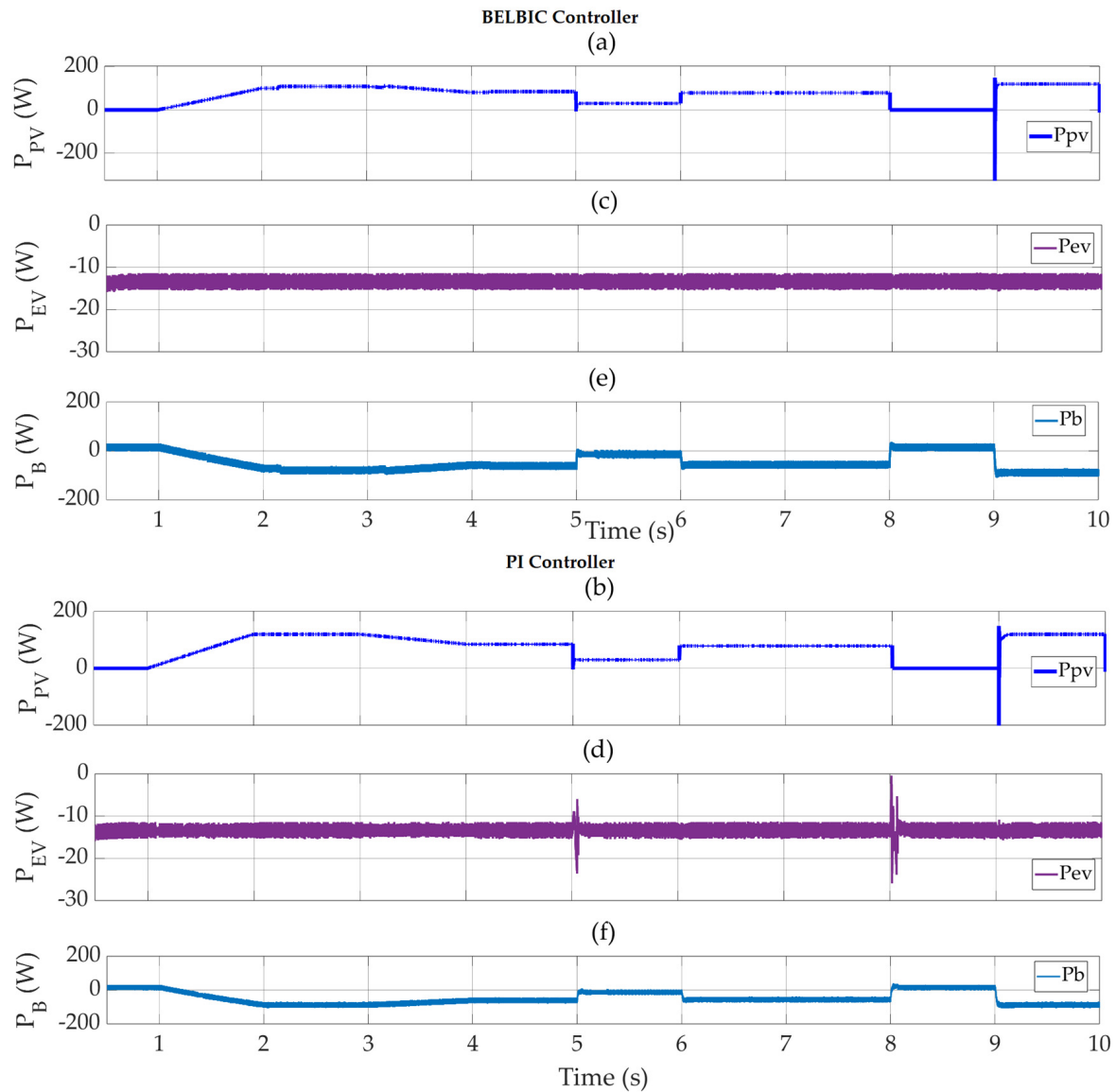
Figure 8. The system power using the suggested BELBIC controller (**a**,**c**,**e**) and the PI controller (**b**,**d**,**f**).

The response of the EV charging process with the suggested BELBIC controller in contrast to the traditional PI controller is seen in Figure 9. The EV's current for both controllers in Figure 9a,b closely resembles the reference that the EV's converter controller produces. Its reaction, however, is better without any ripples or overshoots when using the recommended BELBIC controller. Figure 9c,d demonstrate the voltage of the battery of the EV for each controller. It is noted that the responses do not change as the EV battery keeps charging. The state of charge (SOC) of the battery of the EV using both controllers is shown in Figure 9e,f, respectively. The responses do not change as the EV battery keeps charging for all periods. Except for some switching spikes in the EV battery voltage and current, the two controllers have identical responses. However, the best responses are those with the BELBIC controller.
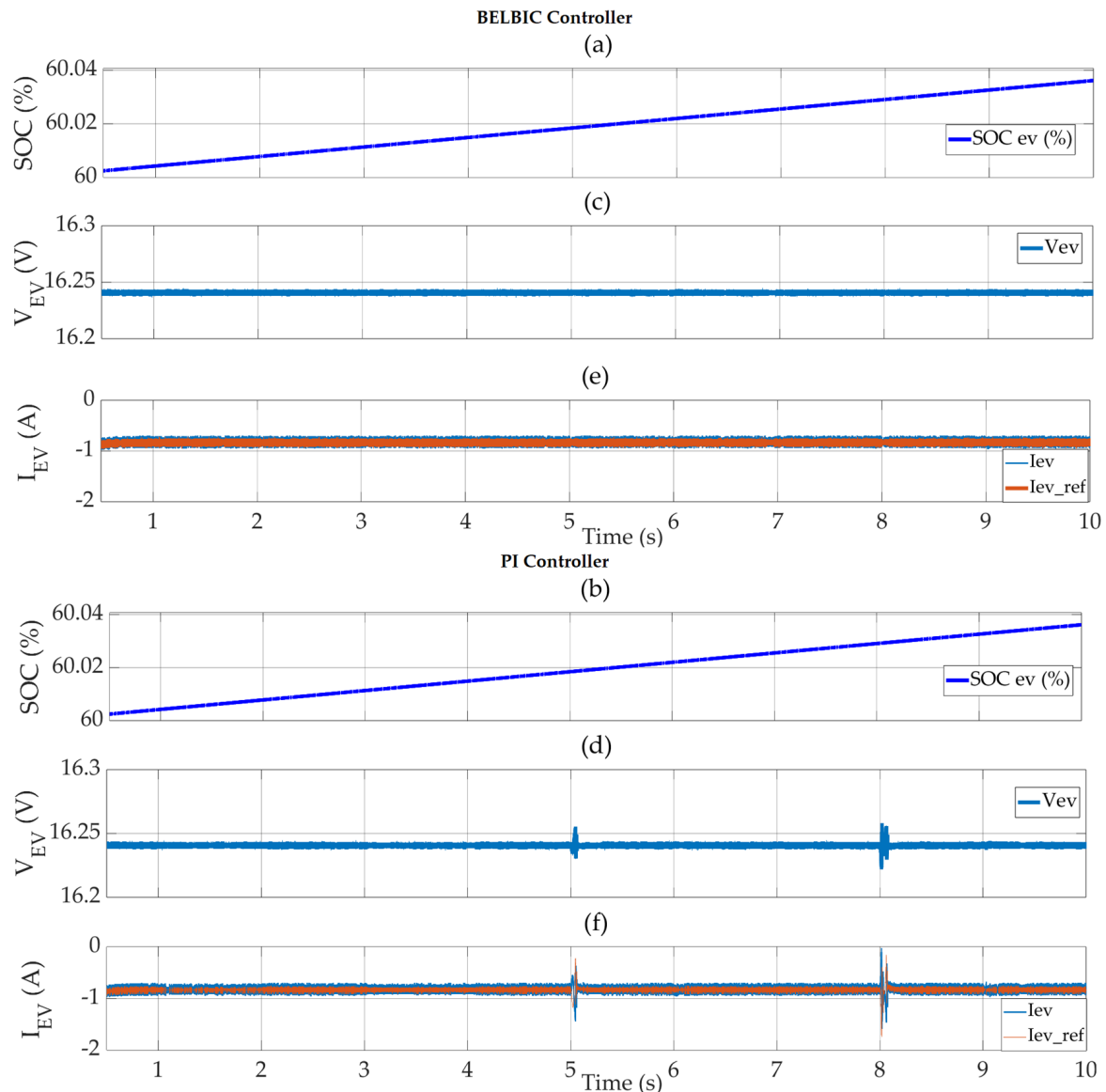
Figure 9. The EV charging performance using the suggested BELBIC controller (**a**,**c**,**e**) and the PI controller (**b**,**d**,**f**).

Figure 10a,b display the SOC response of the storage battery for the suggested BELBIC and conventional PI controllers. For both controllers, the SOC's reaction is almost the same. For the initial second, [1 s to 2 s], the insolation increases linearly, and so does the generated PV energy. The PV energy generated may therefore be used to fully charge the battery of the EV and save any leftover energy in the storage battery. The insolation in the next second, from [2 s to 3 s], is 100%, which is adequate to supply energy to the EV and save the rest in the storage battery. In the next three to four seconds, the insolation decreases linearly to 70% insolation. Hence, the stored energy decreases linearly while the EV charging is constant. In the period from 4 to 5 s, the insolation is around 70%. As a result, the produced PV power may be used to supply energy to the EV battery and save the rest in the storage battery. However, for the next second, from 5 to 6 s, there is only 25% insolation, which is not enough to power the EV with the required energy. Hence, the storage battery empties to balance the decrease in PV-generated power. During the next interval [6 s < t < 8 s], the insolation is 65%, which is not enough to supply energy to the battery of the EV and maintain the remaining energy in the storage battery. As a result, the state of charge slopes modestly and positively. The solar irradiation eventually vanishes through the [8 s–9 s]

interval. During the final period, [9 s–10 s], the insolation steps to 100%, which is a large step. The operation returns to the previous case. Consequently, no power is produced. Hence, to offset the solar energy, the storage battery discharges. The voltage of the storage battery for the suggested BELBIC and conventional PI controllers is shown in Figure 10c,d. Its voltage increases when charged, and decreases when discharged. The current response of the storage battery for both controllers is shown in Figure 10e,f. It tracks its reference quite well for both controllers. The reference value for the current of the storage battery is generated by the DC bus voltage controller. Along with tracking their references, the charging and discharging processes also consider radiation variations.
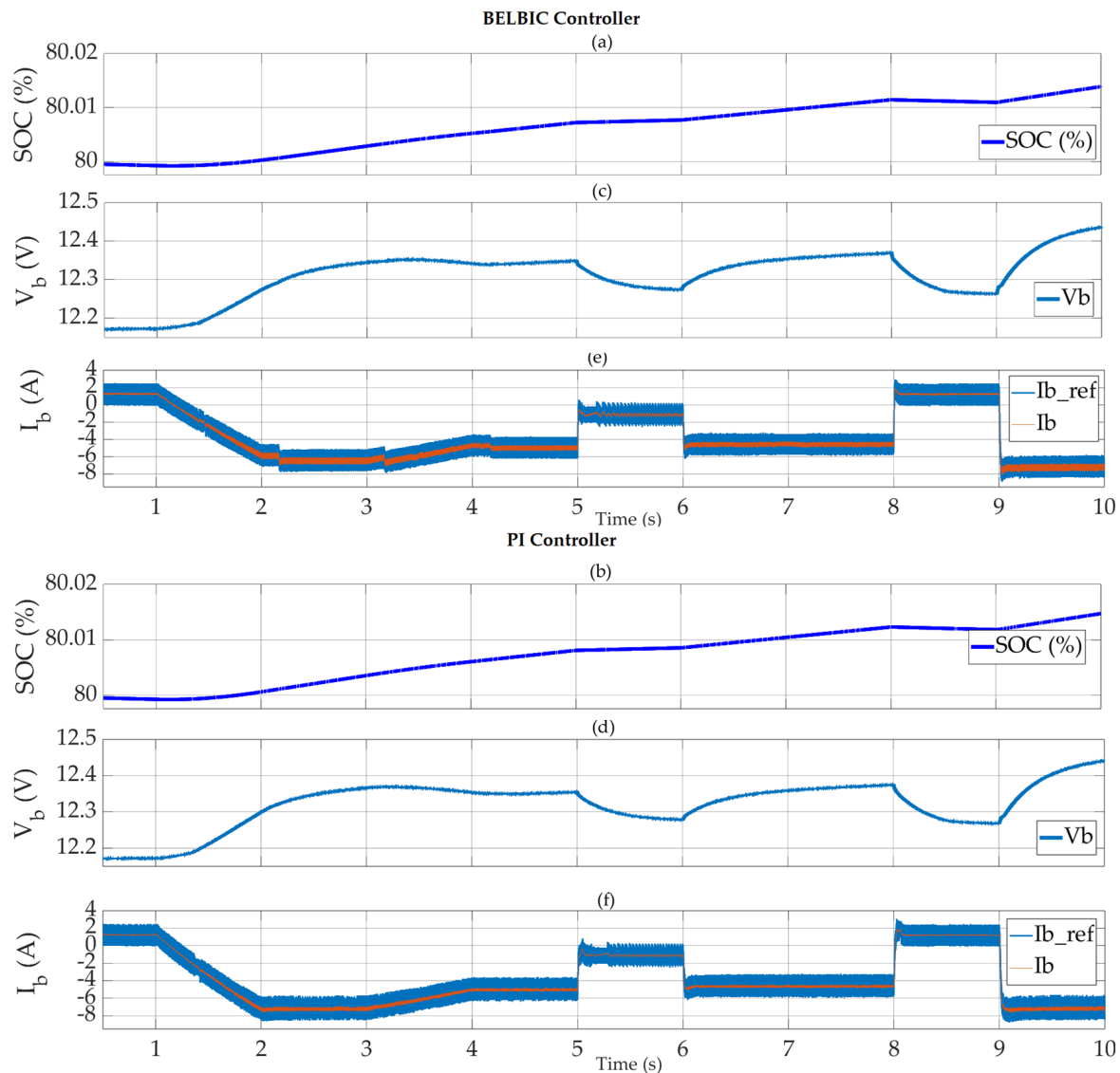

Figure 10. The storage battery performance using the suggested BELBIC controller (**a**,**c**,**e**) and the PI controller (**b**,**d**,**f**).

Figure 11 illustrates how the response of the DC bus voltage with the recommended controller is affected by a $\pm10\%$ difference in the values of the passive components (C_d, L). This is performed to evaluate the BELBIC controller's robustness to parameter mismatches. It is noted that the controller successfully tracks the reference signal, which in such a way illustrates how resistant the control system is to mismatched parameters. Conversely, there is a minor increase in overshoots, but a tiny decrease in ripples.
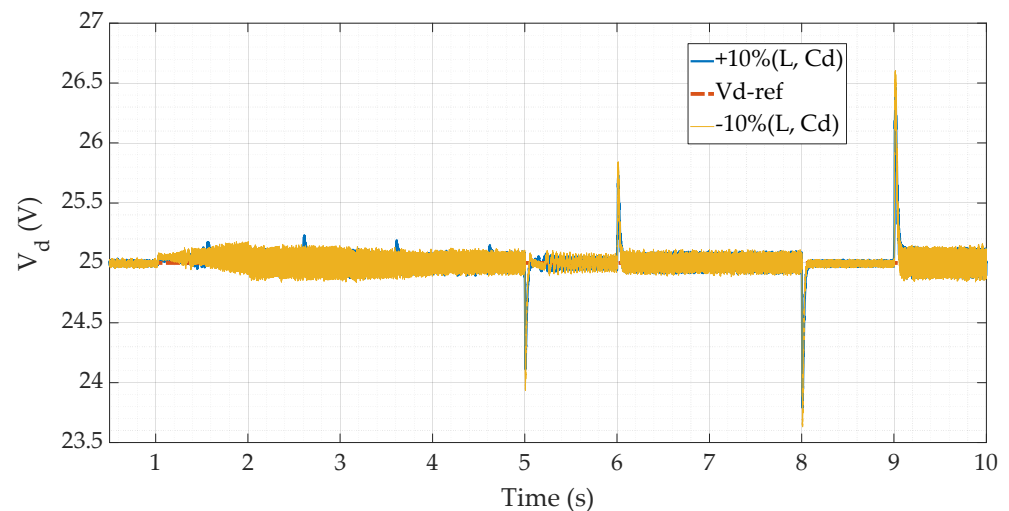
Figure 11. The DC bus voltage response's impact against passive parameter variations.

5. Conclusions

This research aims to provide a novel autonomous PV energy source-powered EV charging station. A PV panel, a step-up converter, a storage battery, an EV battery, and two charging DC/DC converters are some of the parts that make up the suggested system. The control system consists of three controllers: a battery storage controller, an EV charger controller, and a maximum power point tracking controller. These controllers work together to guarantee effective functioning. Even in the face of fluctuating sunshine levels, the battery controller's dual-loop control technology employs the BELBIC approach to provide a steady DC bus voltage for the EV charging station. Utilizing MATLAB and the suggested BELBIC controller, a simulation was run to evaluate the viability of the suggested EV charging station. Regardless of the quantity of sunlight, the EV battery charged steadily, and the storage battery, with the help of the suggested BELBIC controller, efficiently saved energy and adjusted for fluctuations in PV insolation. Also, the suggested BELBIC controller minimized the DC link's voltage overshoot during variations in sunlight by around 50%, in contrast to the conventional PI controller. The settling time was also reduced by 60%. The voltage and current controllers of the converters operated effectively and precisely as intended. Furthermore, the maximum power point tracking controller efficiently kept the PV at its ideal maximum power settings. Future research can improve the system even further by adding new energy storage technologies. A complete study of the system's stability will be prepared for future research.

Author Contributions: S.A.Z. handled the formal analysis, modeling, and conceptualization; H.A. evaluated and reviewed the paper; and A.E. and A.M.A. helped obtain financing. After reading the published version of the article, all authors have given their approval. All authors have read and agreed to the published version of the manuscript.

Conflicts of Interest: The authors declare no conflicts of interest.

Nomenclature

PV	Photovoltaic
EV	Electric vehicles
BELBIC	Brain-Emotional Learning Intelligent Control
DC	Direct current
AC	Alternating current
V_d, I_d	DC link voltage and current
d	Duty ratio of the boost converter
V_{pv}, I_{pv}	PV voltage and current
V_b, I_b	Battery voltage and current
R_s, R_p	panel equivalent series and parallel resistances
I_{SC}	PV short circuit current
L, C	Filter inductance and capacitance
C_d	DC bus capacitance
E_b, r_b	Battery internal voltage and resistance
Q_1, Q_2	Modulating functions of the IGBTs
MO	The net output of the BELBIC controller
A_l, O_l	Amygdala and orbitofrontal cortex outputs
ES	Emotional signals
S	Sensory input
A_{th}	Thalamus node
l	Number of sensory inputs
(G_l and W_l)	Weighting parameters of the amygdala and orbitofrontal cortex
(α and β)	Rate of learning of the amygdala and orbitofrontal cortex
e	Error
y	Plant output
r	Reference signal
u	Control effort output
SOC	State of charge

References

1. Safayatullah, M.; Elrais, M.T.; Ghosh, S.; Rezaii, R.; Batarseh, I. A Comprehensive Review of Power Converter Topologies and Control Methods for Electric Vehicle Fast Charging Applications. *IEEE Access* **2022**, *10*, 40753–40793. [CrossRef]
2. Rajendran, G.; Vaithilingam, C.A.; Misron, N.; Naidu, K.; Ahmed, M.R. A comprehensive review on system architecture and international standards for electric vehicle charging stations. *J. Energy Storage* **2021**, *42*, 103099. [CrossRef]
3. Li, L.; Wang, Z.; Gao, F.; Wang, S.; Deng, J. A family of compensation topologies for capacitive power transfer converters for wireless electric vehicle charger. *Appl. Energy* **2020**, *260*, 114156. [CrossRef]
4. Zaid, S.A.; Bakeer, A.; Albalawi, H.; Alatwi, A.M.; AbdelMeguid, H.; Kassem, A.M. Optimal Fractional-Order Controller for the Voltage Stability of a DC Microgrid Feeding an Electric Vehicle Charging Station. *Fractal Fract.* **2023**, *7*, 677. [CrossRef]
5. Ahmad, F.; Iqbal, A.; Asharf, I.; Marzband, M.; Khan, I. Placement and Capacity of EV Charging Stations by Considering Uncertainties with Energy Management Strategies. *IEEE Trans. Ind. Appl.* **2023**, *59*, 3865–3874. [CrossRef]
6. Yap, L. Electric Car Charging Tips. 2023. Available online: https://www.greencars.com/greencars-101/electric-car-charging-tips (accessed on 1 April 2024).
7. Minh, P.V.; Quang, S.L.; Pham, M.H. Technical Economic Analysis of Photovoltaic-Powered Electric Vehicle Charging Stations under Different Solar Irradiation Conditions in Vietnam. *Sustainability* **2021**, *13*, 3528. [CrossRef]
8. Liu, Y.; Dong, H.; Wang, S.; Lan, M.; Zeng, M.; Zhang, S.; Yang, M.; Yin, S. An Optimization Approach Considering User Utility for the PV-Storage Charging Station Planning Process. *Processes* **2020**, *8*, 83. [CrossRef]
9. Shariff, S.M.; Alam, M.S.; Ahmad, F.; Rafat, Y.; Asghar, M.S.J.; Khan, S. System Design and Realization of a Solar-Powered Electric Vehicle Charging Station. *IEEE Syst. J.* **2020**, *14*, 2748–2758. [CrossRef]
10. Rafi, M.A.H.; Bauman, J.A. Comprehensive Review of DC Fast Charging Stations with Energy Storage: Architectures, Power Converters, and Analysis. *IEEE Trans. Transp. Electrif.* **2021**, *7*, 345–368. [CrossRef]
11. Mouli, C.G.R.; Schijffelen, J.; Heuvel, M.; Kardolus, M.; Bauer, P. A 10 kW Solar-Powered Bidirectional EV Charger Compatible with Chademo and COMBO. *IEEE Trans. Power Electron.* **2019**, *34*, 1082–1098. [CrossRef]
12. Atawi, I.E.; Hendawi, E.; Zaid, S.A. Analysis and Design of a Standalone Electric Vehicle Charging Station Supplied by Photovoltaic Energy. *Processes* **2021**, *9*, 1246. [CrossRef]
13. Awad, M.; Ibrahim, A.M.; Alaas, Z.M.; El-Shahat, A.; Omar, A.I. Design and analysis of an efficient photovoltaic energy-powered electric vehicle charging station using perturb and observe MPPT algorithm. in Front. *Energy Res.* **2022**, *10*, 969482. [CrossRef]

14. Singh, S.; Chauhan, P.; Singh, N.J. Feasibility of grid-connected solar-wind hybrid system with electric vehicle charging station. *J. Mod. Power Syst. Clean Energy* **2020**, *9*, 295–306. [CrossRef]

15. Ahmadi, M.; Kaleybar, H.J.; Brenna, M.; Castelli-Dezza, F.; Carmeli, M.S. DC Railway Micro Grid Adopting Renewable Energy and EV Fast Charging Station. In Proceedings of the 2021 IEEE International Conference on Environment and Electrical Engineering and 2021 IEEE Industrial and Commercial Power Systems Europe (EEEIC/I&CPS Europe), Bari, Italy, 7–10 September 2021; pp. 1–6.

16. Oulad-Abbou, D.; Doubabi, S.; Rachid, A.; García-Triviño, P.; Fernández-Ramírez, L.M.; Fernández-Ramírez, C.A.; Sarrias-Mena, R. Combined control of MPPT, output voltage regulation and capacitors voltage balance for three-level DC/DC boost converter in PV-EV charging stations. In Proceedings of the 2018 International Symposium on Power Electronics, Electrical Drives, Automation and Motion (SPEEDAM), Amalfi, Italy, 20–22 June 2018; pp. 372–376.

17. Sharma, P. Design of novel BELBIC controlled semi-active suspension and comparative analysis with passive and PID controlled suspension. *Walailak J. Sci. Technol.* **2021**, *18*, 8989. [CrossRef]

18. Ershadi, M.H.; Shojaeian, S.; Keramat, R. A comparison of fuzzy and brain emotional learning-based intelligent control approaches for a full bridge DC-DC converter. *Int. J. Ind. Electron. Control. Optim.* **2019**, *2*, 197–206.

19. Zirkohi, M.M. Stability analysis of brain emotional intelligent controller with application to electrically driven robot manipulators. *IET Sci. Meas. Technol.* **2020**, *14*, 182–187. [CrossRef]

20. Sharma, P.; Kumar, V. Design and analysis of novel bio inspired BELBIC and PSOBELBIC controlled semi active suspension. *Int. J. Veh. Perform.* **2020**, *6*, 399–424. [CrossRef]

21. Kumar, G.B. Optimal power point tracking of solar and wind energy in a hybrid wind solar energy system. *Int. J. Energy Environ. Eng.* **2021**, *13*, 77–103. [CrossRef]

22. Karan, D.; Harish, V.S.K.V. Analysis of a wind-PV battery hybrid renewable energy system for a dc microgrid. *Mater. Today Proc.* **2021**, *46*, 5451–5457.

23. Al Alahmadi, A.A.; Belkhier, Y.; Ullah, N.; Abeida, H.; Soliman, M.S.; Khraisat, Y.S.H.; Alharbi, Y.M. Hybrid wind/PV/battery energy management-based intelligent non-integer control for smart DC-microgrid of smart university. *IEEE Access* **2021**, *9*, 98948–98961. [CrossRef]

24. Hua, M.; Zhang, C.; Zhang, F.; Li, Z.; Yu, X.; Xu, H.; Zhou, Q. Energy management of multi-mode plug-in hybrid electric vehicle using multi-agent deep reinforcement learning. *Appl. Energy* **2023**, *348*, 121526. [CrossRef]

25. Kouro, S.; Cortés, P.; Vargas, R.; Ammann, U.; Rodríguez, J. Model predictive control—A simple and powerful method to control power converters. *IEEE Trans. Ind. Electron.* **2008**, *56*, 1826–1838. [CrossRef]

26. Şahin, M.E.; Blaabjerg, F. A Hybrid PV-Battery/Supercapacitor System and a Basic Active Power Control Proposal in MAT-LAB/Simulink. *Electronics* **2020**, *9*, 129. [CrossRef]

27. Sharaf, A.M.; Şahin, M.E. A Flexible PV-Powered Battery-Charging Scheme for Electric Vehicles. *IETE Tech. Rev.* **2017**, *34*, 133–143. [CrossRef]

28. Zaid, S.A.; Albalawi, H.; Alatawi, K.S.; El-Rab, H.W.; El-Shimy, M.E.; Lakhouit, A.; Alhmiedat, T.A.; Kassem, A.M. Novel Fuzzy Controller for a Standalone Electric Vehicle Charging Station Supplied by Photovoltaic Energy. *Appl. Syst. Innov.* **2021**, *4*, 63. [CrossRef]

29. Rashid, M. *Power Electronics Handbook*, 2nd ed.; Elsevier Press: Amsterdam, The Netherlands, 2011.

30. Şahin, M.E.; Blaabjerg, F. PV Powered Hybrid Energy Storage System Control Using Bidirectional and Boost Converters. *Electr. Power Comp. Syst.* **2021**, *49*, 1260–1277. [CrossRef]

31. Zaid, S.A.; Kassem, A.M. Review, analysis and improving the utilization factor of a PV-grid connected system via HERIC transformerless approach. *Renew. Sustain. Energy Rev.* **2017**, *73*, 1061–1069. [CrossRef]

32. Albalawi, H.; El-Shimy, M.E.; AbdelMeguid, H.; Kassem, A.M.; Zaid, S.A. Analysis of a Hybrid Wind/Photovoltaic Energy System Controlled by Brain Emotional Learning-Based Intelligent Controller. *Sustainability* **2022**, *14*, 4775. [CrossRef]

33. Jafari, M.; Xu, H.; Carrillo, L.R.G. Brain emotional learning-based intelligent controller for flocking of multi-agent systems. In Proceedings of the 2017 American Control Conference (ACC), Seattle, WA, USA, 24–26 May 2017; pp. 1996–2001.

34. Muthusamy, P.K.; Garratt, M.; Pota, H.; Muthusamy, R. Real-time adaptive intelligent control system for quadcopter unmanned aerial vehicles with payload uncertainties. *IEEE Trans. Ind. Electron.* **2021**, *69*, 1641–1653. [CrossRef]

35. Yeganeh, M.S.O.; Oshnoei, A.; Mijatovic, N.; Dragicevic, T.; Blaabjerg, F. Intelligent secondary control of islanded AC microgrids: A brain emotional learning-based approach. *IEEE Trans. Ind. Electron.* **2022**, *70*, 6711–6723. [CrossRef]

36. Dorrah, H.T.; El-Garhy, A.M.; El-Shimy, M.E. PSO-BELBIC scheme for two-coupled distillation column process. *J. Adv. Res.* **2011**, *2*, 73–83. [CrossRef]